PATHOGENICITY ASSESSMENT AND GENOMIC CHARACTERIZATION OF BACTERIAL LEAF SPOT ISOLATES FROM SUGARBEET LEAF SAMPLES IN 2025

Jacob Fjeld[1], Tsebaot Getachew[1], James Deleon[2] Austin K. Lien[3] and Ashok K. Chanda[4]

[1]Undergraduate Laboratory Assistant, University of Minnesota Crookston, Crookston, MN; [2]Laboratory Technician, Northwest Research and Outreach Center, Crookston, MN; [3]Research Professional 3, Northwest Research and Outreach Center, Crookston, MN; [4]Associate Professor & Extension Sugarbeet Pathologist, University of Minnesota, Department of Plant Pathology, St. Paul, MN & Northwest Research and Outreach Center, Crookston, MN

Corresponding Author: Ashok Chanda, achanda@umn.edu

INRODUCTION

Bacterial leaf spot (BLS) is a damaging foliar disease, primarily caused by *Pseudomonas syringae* and *Xanthomonas campestris*, two gram-negative bacterial pathogens capable of infecting lettuce, cucurbits, tomatoes, capsicum, beets, spring onions, and other crops (Xin et al. 2018; Gaetán and López 2005; Saxena et al. 2020). These pathogens enter plant tissues through stomata, hydathodes, or wounds and colonize the mesophyll parenchyma, where they release type III effector proteins that suppress salicylic-acid-mediated defense signaling (Üstün et al. 2013; Xin et al. 2018). As bacterial populations expand, cells emerge onto the leaf surface where they disperse by rain or wind, increasing epidemic potential (An et al. 2019; Moreira et al. 2014). Seedborne transmission further enables long-distance spread and recurrent outbreaks (An et al. 2019). Symptoms of BLS typically develop as water-soaked lesions surrounded by chlorosis, progressing to necrosis driven by plant immune responses or bacterial phytotoxins (Osdaghi et al. 2021; Abrahamian et al. 2020). Environmental conditions play a major role in disease progression; warm temperatures (20-30°C) and high humidity create optimal conditions for rapid symptom development (Vidaver and Lambrecht 2004; Gaulke and Goldman 2022).

Historically, BLS has been documented for over a century, with early descriptions reported in nasturtium and sugar beet in the early 1900s (Journal of Agricultural Research 1913). Recent decades have seen increasing outbreaks, expanded host ranges, and the emergence of antibiotic resistance. For example, new lineages of *Xanthomonas perforans* have recently caused severe outbreaks in peppers (Subedi et al. 2023), while the strAB streptomycin-resistance gene now occurs across several major plant pathogens including *P. syringae* and *X. campestris* (Sundin and Wang 2018). Management strategies such as application of copper and streptomycin sprays, and seed treatments with heat or chemicals, are becoming less effective as resistance increases (Cooksey 1990; Pernezny et al. 2002; Macnish 1965). Given this trend, there is a critical need for improved genomic characterization and pathogenicity validation of emerging BLS-associated bacteria. In this study, bacteria were isolated from symptomatic sugarbeet leaf samples, tested for their pathogenicity using controlled inoculation assays, and whole-genome sequencing and phylogenetic analysis were performed to identify species and evolutionary relationships. The resulting dataset provides insights into the pathogenic potential and genomic identity of these field-recovered bacterial isolates.

OBJECTIVES

The objectives of this study were to 1) conduct preliminary phylogenic analyses to determine genus-level identification of 34 bacterial isolates collected from leaf samples submitted to the Sugarbeet Plant Pathology lab in 2024; 2) carry out a trial within a controlled environment chamber to assess the pathogenicity of 20 bacterial isolates using three sugar beet cultivars; and 3) perform whole genome sequencing of the 20 isolates used in the pathogenicity assay to determine species level identification.

MATERIALS AND METHODS

Bacterial isolation and preliminary phylogenetics. A total of 14 leaf samples exhibiting BLS-like symptoms (Fig. 1) were submitted to the Sugar Beet Plant Pathology Laboratory between July and August 2024 (Table 1). Leaf spots that lacked visible fungal sporulation were tested for bacterial streaming by submerging symptomatic tissue in ultrafiltered deionized water and observing for exudate under a stereomicroscope. Suspect lesions were then excised, surface-sterilized in 0.5% sodium hypochlorite (NaOCl) for 1 m, rinsed thrice with sterile deionized water (SDW),

and homogenized in 0.05M potassium phosphate buffer within 2 mL microcentrifuge tubes containing five 3 mm-glass beads using a FastPrep-24 homogenizer (MP Biomedicals). After incubation at room temperature for 10 m, the suspension was diluted 1:10 in SDW and streaked onto nutrient broth yeast extract (NBY) agar amended with cycloheximide (750 mg L^{-1}) to obtain single bacterial colonies. Single-colony cultures were grown in nutrient broth in 15 mL sterile conical tubes at 28°C on a shaker overnight prior to genomic DNA (gDNA) extraction. After 48 hours, saturated liquid cultures were combined 1:2 with glycerol solution (65% glycerol, 0.1 M $MgSO_4$, 25 mM Tris-Cl, pH 8.0) and stored at -80°C in 2 mL cryovials. Genomic DNA was extracted using the Wizard Genomic DNA purification kit (Promega) following the manufacturer's protocol. The concentration of gDNA was evaluated using Qubit 3.0 fluorometer using the high sensitivity assay kit and gDNA quality was assessed with a NanoDrop spectrophotometer.

Isolates were subjected to targeted sequencing of the *16S-23S* ribosomal RNA (rRNA) intergenic region (Guasp et al. 2000; Jensen et al. 1993) and housekeeping genes sigma factor 70 subunit, *rpoD*; and gyrase B, *gyrB* (Sarkar and Guttman 2004) for genus-level characterization. PCR reactions were performed in a total volume of 30 µL and consisted of 3 ng gDNA, 2X GoTaq Colorless Master Mix (Promega), 10 µM of forward and reverse primers. Amplifications were carried out on a Bio-Rad T100™ Thermal Cycler. The PCR conditions for the *16S-23S* rRNA primers were 94°C for 5 m for initial denaturation, followed by 30 cycles of denaturation at 94°C for 1 min, annealing at 55°C for 1 min, and extension 72°C for 2 min, with a final extension at 72°C for 10 min. The PCR conditions for the *rpoD* primers were 94°C for 3 m for initial denaturation, followed by 30 cycles of denaturation at 94°C for 2 m, annealing at 62°C for 30 s, and extension 72°C for 1 min, with a final extension at 72°C for 5 m. The PCR conditions for the *gyrB* primers were 94°C for 5 m for initial denaturation, followed by 35 cycles of denaturation at 94°C for 2 min, annealing at 63°C for 1 min, and extension 72°C for 1 min, with a final extension at 72°C for 5 min. All amplified DNA products were loaded on 1.5% agarose gel amended with 1X GelRed nucleic acid stain (Millipore, USA) to confirm PCR amplification.

The amplified DNA products were submitted to Molecular Cloning Laboratories (South San Fransico, CA) for PCR clean-up and Sanger sequencing. Sequence chromatograms were reviewed, reads were manually trimmed, and forward and reverse sequences were aligned in BioEdit v7.7.1. Contiguous sequences were compared to the NCBI database using the Nucleotide Basic Local Alignment Search Tool (BLASTn), optimized for highly similar sequences. Reference sequences with high similarity were downloaded from NCBI to be included in the phylogenetic analysis. Phylogenetic analyses were performed in R (v4.4.3; R Core Team 2025). FASTA files were imported using Biostrings (v2.74.1; Pagès et al. 2024). Sequences were oriented and aligned using DECIPHER (v3.2.0; Wright 2016), and pairwise genetic distances were calculated using seqinr (v4.2-36; Charif and Lobry 2007). Phylogenetic trees were constructed using phangorn (v2.12.1; Schliep 2011) with the UPGMA algorithm and visualized using ggtree (v3.14.0; Guangchuang et al. 2017). Based on the preliminary phylogenetic placement and survivability after storage, 20 representative isolates were selected for pathogenicity assays and whole genome sequencing.

Pathogenicity assays. Three sugar beet cultivars, Crystal 912, Crystal 260, and Betaseed 8018, were planted in triplicate for each bacterial isolate, along with two negative controls, a nontreated control (NTC) and a mock control (MC). All seeds were commercially treated with seed treatments of Tachigaren (45g/ unit), Kabina (14g/unit), and standard rates of Allegiance, Thiram, and Poncho Beta. Ten seeds were planted per plastic pot (4.5 x 4.5 x 4 inches); plants were thinned to five plants per pot at the two-leaf stage. Pots were placed in a controlled growth chamber set to maintain 65% relative humidity with a 14-hour photoperiod using LED grow lights (LumiGrow) at 25 + 2 °C and watered approximately every other day.

This experiment was conducted as a series of three sequential pathogenicity assays, each structured as a split-plot design. A split-plot layout was used to account for possible differences within the growth chamber (e.g., differences in light intensity and airflow between positions). Isolates were blocked by replicate, and cultivars were used as whole plots to minimize environmental effects associated with specific chamber positions. In the first assay, 10 isolates were evaluated; a second assay evaluated an additional 10 isolates using the same design. Based on disease severity results from assays 1 and 2, the 10 most virulent isolates were re-evaluated in a third assay to confirm pathogenicity. The total number of infiltrations per isolate (across one or two assays) is reported in Table 2.

Cultures retrieved from storage were streaked onto NBY agar and incubated for 48 hours at 28°C. A single colony was streaked onto new NBY agar and incubated for 48 hours at 28°C. Six milliliters of SDW was added to each

plate, cells were dislodged using a stainless-steel spreader, and the suspension was collected into 15 mL sterile conical tubes and adjusted to a final volume of 10 mL with SDW. Bacterial suspensions were quantified using a spectrophotometer with 200 µL per cuvette and diluted to an optical density of OD_{600} = ~0.9, corresponding to approximately 1 x 10^8 colony forming units (CFU) per mL. The number of CFUs was determined by further dilution (1:100,000) into SDW and spreading 100 µL of the suspension onto NBY agar. Following an incubation period of 48 hours at 28°C, individual colonies were manually counted to obtain CFU mL^{-1}.

Infiltrations were conducted at the 4-leaf stage using 1 cc of inoculum administered with a needleless syringe. One leaf per plant received two to four infiltration sites spaced 1 cm apart, resulting in approximately 18 infiltrations per cultivar x isolate x replicate. The petiole of each inoculated leaf was marked with a red felt-tipped marker. The growth chamber was adjusted to maintain a relative humidity at or greater than 85% and temperature of 25 + 2 °C for 96 hours following infiltrations. Bacterial leaf spot severity was assessed at 7 and 14 days after infiltration (DAI) using a 0-4 scale in which 0 = no visible symptoms, 1 = slight chlorosis, 2 = moderate chlorosis or bleaching, 3 = slight necrosis, 4 = moderate to severe necrosis or cell death. Severity scores were converted into a quantitative disease severity index (DSI) ranging from 0 to 100. To calculate DSI, the number of infiltration sites assigned to each severity rating (0-4) was multiplied by its corresponding rating value, and these products were summed and divided by the maximum possible disease score (i.e., total number of sites × 4). This proportion was then multiplied by 100 to produce a standardized DSI value. A DSI of 100 indicates that all infiltration sites exhibited severe necrosis (i.e., rating = 4).

A combined statistical analysis was performed in R (v 4.3.1, R Core Team 2023) to elucidate treatment interactions and account for variability between individual assays. The package agricolae (v 1.3-7; de Mendiburu 2023) was used to perform a mixed model ANOVA that reflected the split-plot trial design using the sp.plot argument. Main plots (sugar beet cultivars) and subplots (bacterial isolates) were treated as fixed effects. Replication within assay was assigned as the random effect and the main-plot error term was derived from the replication*main plot interaction in the combined analyses. Mean comparisons were conducted according to the Least Significant Difference test using the LSD.test argument at a 0.05 level of significance using the respective error terms for main plots, subplots, and interactions.

On 14 DAI, symptomatic leaf tissue was excised, surface-sterilized in 0.5% NaOCl for 1 m, rinsed thrice with SDW, and homogenized in 0.05M potassium phosphate buffer within 2 mL microcentrifuge tubes containing five 3 mm-glass beads using a FastPrep-24 homogenizer (MP Biomedicals). After incubation at room temperature for 10 m, the suspension was diluted 1:10 in SDW and streaked onto NBY agar amended with cycloheximide (750 mg L^{-1}). Colony morphology was compared to original isolates to fulfill Koch's postulates.

Whole genome sequencing. Cultures taken from storage were streaked onto NBY agar and incubated for 48 hours at 28°C. Single-colony cultures were grown in nutrient broth in 15 mL sterile conical tubes at 28°C on a shaker overnight prior to DNA extraction. Fresh cells were pelleted by centrifugation at 1,000 x *g* for 1 m, the supernatant was removed, and the pellet was resuspended in 100 µL cold phosphate-buffered saline (PBS). High molecular weight gDNA was isolated using the Monarch® Spin gDNA Extraction Kit (New England Biolabs) following the manufacturer's protocol. The concentration of gDNA was evaluated using Qubit 3.0 fluorometer using the high sensitivity assay kit, gDNA quality was assessed with a NanoDrop spectrophotometer, and gDNA integrity was evaluated by loading 60 ng of gDNA on 0.8% agarose gel.

High-quality gDNA was used as input for library preparation with the Oxford Nanopore Rapid PCR Barcoding Kit 24 V14 (SQK-RPB114.24) following the manufacturer's protocol. For each sample, 3 to 5 ng of gDNA was used as starting material for the barcoding reaction. Library preparation, PCR amplification, and clean-up steps were performed according to kit instructions, using the recommended reagent volumes and cycling conditions. All barcoded samples were pooled in equimolar ratios to a combined final concentration of 300 fmol (~600 ng) into a single 1.5 mL tube. The pooled libraries were cleaned using AMPure XP following the kit instructions and responded in 15 uL of elution buffer. Approximately 75 ng of the final pooled libraries were loaded onto an Oxford Nanopore MinION Mk1D device equipped with an R10.4.1 flow cell. Sequencing was performed for 24 hours, after which the flow cell was washed using the Flow Cell Wash Kit according to the manufacturer's protocol. The same pooled libraries were then reloaded, and sequencing was continued for an additional 24 hours.

Raw POD5 files generated by the MinKNOW software were transferred to the Minnesota Supercomputing Institute (MSI) high-performance computing (HPC) system for downstream analysis. Reads were basecalled and demultiplexed using the wf-basecalling workflow (EPI2ME), which produced barcoded FASTQ files for each sample. Demultiplexed reads were then processed using the wf-bacterial-genomes workflow (EPI2ME) to generate genome assemblies and annotations. Assembly was performed with Flye, and consensus polishing was conducted using Medaka. The workflow produced barcoded FASTA assemblies and corresponding GFF annotation files for each sample, as well as antimicrobial resistance predictions. Assembly quality metrics were evaluated using QUAST, which provided summary statistics including N50, total assembly size, number of contigs, and GC content.

RESULTS AND DISCUSSION

Preliminary phylogenetics. A total of 34 bacterial isolates were collected from 14 leaf samples exhibiting BLS-like symptoms in the Red River Valley of Minnesota and southern Minnesota in 2024 (Table 1). Sample submissions spanned multiple counties and townships, indicating that BLS-like symptoms were observed broadly across the region during the 2024 growing season. In certain instances, anecdotal evidence suggests submissions coincided with periods following high wind conditions that had the potential to create leaf wounds, which are conducive to bacterial colonization.

Initial taxonomic identification using the *16S-23S* rRNA intergenic region revealed that field samples contained a distinct *Pseudomonas*-associated clade (clade I), Xanthomonas-associated clade (clade II) as well as a separate *Enterobacterales*-associated cluster (clade III) (Fig. 2).
In clade Ia, a substantial number of isolates clustered with *Pseudomonas putida*, *P. japonica*, and *P. monteilii*. This group corresponds to the *P. putida* lineage, which is phylogenetically distant from the *P. syringae* complex and is composed primarily of environmental or plant-associated epiphytes rather than aggressive foliar pathogens. Clade Ib contained a single isolate that grouped with *Pseudomonas syringae* and *P. syringae pv. aptata*, the historically recognized causal agent of bacterial leaf spot in sugar beet. In clade Ic, *Pseudomonadaceae* lineage consisted of isolates clustering with the former "straminea" group, recently reassigned to the genus *Phytopseudomonas* (Rudra & Gupta 2024) were clustered. Species in this group are generally environmental pseudomonads and are considered weakly or non-pathogenic in plants. In addition to these *Pseudomonas*-associated lineages, a large number of isolates formed a clearly separated clade (clade III) belonging to the *Enterobacterales*, including sequences related to *Pantoea agglomerans*, *Kosakonia cowanii*, *Enterobacter* spp., and *Lelliottia* spp. Members of these genera are common wound-associated colonizers, epiphytes, and opportunistic endophytes, and range ecologically from beneficial symbionts to opportunistic plant pathogens under stress or injury. Their presence suggests a diverse, wound-associated microbiome within the sampled BLS-like lesions. One isolate clustered with *Xanthomonas sacchari*, a species reported primarily as a sugarcane pathogen in clade II; however, little is known about its pathogenicity or host range outside sugarcane (Mielnichuk et al. 2021).

Analysis of BLAST results of the *gyrB* amplicons showed that, in addition to the single isolate (24_26_2) grouped with *P. syringae* pv. *aptata* in the *16S-23S* phylogeny, three additional isolates (24_49_3, 24_CR+_3, 24_CR+_5) displayed high identity (99.7–100%) to *P. syringae pv. aptata* (KM282305.1). For most other isolates, *gyrB* classification was broadly consistent with their placement in the *16S-23S* phylogeny. In contrast, the *rpoD* marker provided limited taxonomic resolution but consistently amplified only *Pseudomonas* DNA, with no amplification from most *Enterobacterales* isolates. This pattern indicates that the *rpoD* primers used here are highly *Pseudomonas*-specific. Moreover, in certain instances, this resulted in the amplification of *Pseudomonas* sequences even when the cultured isolate belonged to an unrelated genus. Such primer bias highlights an important limitation of single-locus PCR diagnostics in polymicrobial field samples.

Pathogenicity assays. Symptoms first developed approximately 3 DAI, with no rapid necrosis or water-soaking typical of a Type III secretion system (T3SS)–mediated hypersensitive response. Ratings were conducted on 7 and 14 DAI. By 14 DAI, older leaves began to senesce, indicating that plants were becoming pot-bound and the assay could not be extended beyond this point. There were no significant interactions between sugar beet cultivar and bacterial isolate for DSI or incidence at either evaluation date (Table 2). Similarly, no significant differences were detected among the three sugar beet cultivars at 7 DAI, with DSI values and incidence ranging from 18.3 to 20.1 and 50% to 51%, respectively. Non-significant differences among sugar beet cultivars persisted, with DSI values ranging from 28.4 to 30.7, and incidence was 68% at14 DAI. The lack of differences indicated that cultivar response did not influence disease development under the infiltration conditions used in this study.

In contrast, there were highly significant ($P < 0.0001$) differences among bacterial isolates for both DSI and incidence at 7 and 14 DAI. The mock control exhibited slight discoloration and mild chlorosis, consistent with mechanical damage from infiltration, but its DSI did not differ significantly from the nontreated control at either rating date. Across isolates, DSI values ranged from 8.3 to 33.4 at 7 DAI, with incidence ranging from 30% to 76%. By 14 DAI, disease severity increased for nearly all isolates, with DSI values ranging from 16.9 to 44.4 and incidence from 49% to 91%. Several isolates (24_43_2, 24_CR_1, 24_CR_3, and 24_46_1) consistently produced the highest DSI values at both rating dates, whereas others induced minimal symptom development (e.g., 24_35_5 and 24_35_2).

The delay in initial symptom development, coupled with the gradual onset of chlorosis and localized necrosis, suggests that most isolates caused symptoms primarily through wound colonization and opportunistic growth, rather than through delivery of T3SS effector proteins into host cells. The ability of most isolates to induce mild to moderate chlorosis after syringe infiltration is consistent with previous reports indicating necrosis can occur when bypassing natural infection barriers. The pathogenicity results therefore support the conclusion that a diverse wound-associated microbiome was present in BLS-like lesions.

Whole genome sequencing. Long-read sequencing of the 20 bacterial isolates generated high-coverage datasets with median read qualities ranging from Q25.92 to Q26.52 and median read lengths between 2.19 and 4.65 kb. Total sequencing yield per barcode ranged from 51 Mb to 1240 Mb, with a mean of 910 Mb, providing sufficient depth for complete or near-complete genome assembly for all isolates. Coverage across assemblies ranged from 58X to 319X, well above the minimum threshold required for reliable consensus polishing. Genome assembly metrics varied among isolates, reflecting differences in genome size and genomic complexity. Assemblies ranged from 0.75 Mb to 5.51 Mb, with most isolates producing genome sizes consistent with *Enterobacterales* or *Pseudomonadaceae*. The number of contigs per assembly ranged from 3 to 193, with N50 values ranging from 11.7 kb to 4.8 Mb, indicating high assembly contiguity for most isolates. GC content ranged from 47.3% to 61.4%, consistent with the diversity of bacterial lineages recovered. Several isolates carried predicted antimicrobial resistance genes, including fosA2, OqxA/OqxB efflux pump components, blaERP-1, blaRAHN-2, and blaACT-12. These genes are commonly observed in environmental *Enterobacterales* and may reflect the ecological backgrounds of the isolates. Across nearly all samples, assembly quality was robust, had high coverage, and large N50 values, providing a strong foundation for downstream taxonomic and comparative genomic analyses.

ACKNOWLEDGEMENTS

We thank the Sugarbeet Research and Education Board of Minnesota and North Dakota for funding this research; Crystal Beet Seed and Betaseed for providing seed; the University of Minnesota Northwest Research and Outreach Center for providing equipment and other facilities.

LITERATURE CITED

Sarkar SF, Guttman DS. 2004. Evolution of the core genome of *Pseudomonas syringae*, a highly clonal, endemic plant pathogen. Appl. Environ. Microbiol. 74(6): 1961. https://doi.org/10.1128/AEM.70.4.1999-2012.2004

Guasp C, Moore ER, Lalucat J, Bennasar A. 2000. Utility of internally transcribed 16S-23S rDNA spacer regions for the definition of *Pseudomonas stutzeri* genomovars and other *Pseudomonas* species. International Journal of Systematic and Evolutionary Microbiology. 50(4):1629–1639. https://doi.org/10.1099/00207713-50-4-1629

Jensen MA, Webster JA, Straus N. 1993. Rapid identification of bacteria on the basis of polymerase chain reaction-amplified ribosomal DNA spacer polymorphisms. Appl. Environ. Microbiol. 59(4): 945-952. https://doi.org/10.1128/aem.59.4.945-952.1993

Subedi A, de la Barrera LB, Ivey ML, Egel DS, Kebede M, Kara S, Aysan Y, Minsavage GV, Roberts PD, Jones JB, Goss EM. 2023. Population Genomics Reveals an Emerging Lineage of *Xanthomonas perforans* on Pepper. Phytopathology. 114(1):241-250. https://doi.org/10.1094/phyto-04-23-0128-r

Saxena A, Rai D, Kalra A, Saxena MJ. 2020. Bacterial Diseases of Crops: Epidemiology, Symptoms and Management. Int. J. Curr. Microbiol. App. Sci. 9(06): 1483-1499. https://doi.org/10.20546/ijcmas.2020.906.183

Abrahamian P, Sharma A, Jones J, Vallad GE. 2020. Dynamics and spread of bacterial spot epidemics in tomato transplants grown for field production. Plant Disease. 105(3):566-575. https://doi.org/10.1094/pdis-05-20-0945-re

An S-Q, Potnis N, Dow M, Vorhölter F-J, He Y-Q, Becker A, Teper D, Li Y, Wang N, Bleris L, et al. 2019. Mechanistic insights into host adaptation, virulence and epidemiology of the phytopathogen Xanthomonas. FEMS Microbiology Reviews. 44(1):1-32. https://doi.org/10.1093/femsre/fuz024.

Cooksey DA. 1990. Genetics of bactericide resistance in plant pathogenic bacteria. Annu Rev Phytopathol. 28:201-219.

Gaetán S, López N. 2005. First Outbreak of Bacterial Leaf Spot Caused by Xanthomonas campestris on Canola in Argentina. Plant Disease. 89(6):683-683. https://doi.org/10.1094/pd-89-0683b

Gaulke E, Goldman IL. 2022. Screening table beet and Swiss chard for resistance to Pseudomonas syringae pathovar aptata. HortScience. 57(11):1436-1446. https://doi.org/10.21273/HORTSC116777-22

Janda JM, Abbott SL. 2007. 16S rRNA gene sequencing for bacterial identification in the diagnostic laboratory: Pluses, perils, and pitfalls. Journal of Clinical Microbiology. 45(9):2761-2764

Journal of Agricultural Research. 1913. Washington, D.C.: Dept. of Agriculture. Vol. I, No. 3. p. 189. (Journal of Agricultural Research 1913)

Leandro Márcio Moreira, Agda Paula Facincani, Cristiano Barbalho Ferreira, Ferreira RM, Ferro T, Gozzo FC, Franco C, Jesus Aparecido Ferro, Márcia Regina Soares. 2014. Chemotactic signal transduction and phosphate metabolism as adaptive strategies during citrus canker induction by *Xanthomonas citri*. Functional & Integrative Genomics. 15(2):197–210. https://doi.org/10.1007/s10142-014-0414-z

Macnish G. 1965. Vegetable Seed Treatments. Journal of the Department of Agriculture, Western Australia, Series. 4(12):10. https://library.dpird.wa.gov.au/cgi/viewcontent.cgi?params=/context/journal_agric ulture4/article/3752/&path_info=JAs4v6n121965p721_724.pdf

Nazarov PA, Baleev DN, Ivanova MI, Sokolova LM, Karakozova MV. 2020. Infectious plant diseases: etiology, current status, problems and prospects in plant protection. Acta Naturae. 12(3):46-59. https://doi.org/10.32607/actanaturae.11026

Newberry EA, Ritchie L, Babu B, Sanchez T, Beckham KA, Jones JB, Freeman JH, Dufault NS, Paret ML. 2017. Epidemiology and management of bacterial leaf spot on watermelon caused by *Pseudomonas syringae*. Plant Disease. 101(7):1222-1229. https://doi.org/10.1094/pdis-11-16-1628-re

Osdaghi E, Jones JB, Sharma A, Goss EM, Abrahamian P, Newberry EA, Potnis N, Carvalho R, Choudhary M, Paret ML, et al. 2021. A centenary for bacterial spot of tomato and pepper. Molecular Plant Pathology. 22(12):1500-1519. https://doi.org/10.1111/mpp.13125

Pernezny K, Nagata R, Raid RN, Collins J, Carroll A. 2002. Investigation of Seed Treatments for Management of Bacterial Leaf Spot of Lettuce. Plant Disease. 86(2):151-155. https://doi.org/10.1094/pdis.2002.86.2.151

Ryan RP, Vorhölter F-J, Potnis N, Jones JB, Van Sluys M-A, Bogdanove AJ, Dow JM. 2011. Pathogenomics of *Xanthomonas*: understanding bacterium–plant interactions. Nature Reviews Microbiology. 9(5):344–-355. https://doi.org/10.1038/nrmicro2558

Sundin GW, Wang N. 2018. Antibiotic Resistance in Plant-Pathogenic Bacteria. Annual Review of Phytopathology. 56(1):161-180. https://doi.org/10.1146/annurev-phyto-080417-045946

Üstün S, Bartetzko V, Börnke F. 2013. The *Xanthomonas campestris* Type III Effector XopJ Targets the Host Cell Proteasome to Suppress Salicylic-Acid Mediated Plant Defence. He S, editor. PLoS Pathogens. 9(6):e1003427. https://doi.org/10.1371/journal.ppat.1003427

Vidaver AK, Lambrecht PA. 2004. Bacteria as plant pathogens. Plant Health Instructor. https://doi.org/10.1094/PHI-I-2004-0809-01

Xin X-F, Kvitko B, He SY. 2018. *Pseudomonas syringae*: what it takes to be a pathogen. Nature Reviews Microbiology. 16(5):316-328. https://doi.org/10.1038/nrmicro.2018.17

Milovanović DTP et al. 2025. https://doi.org/10.1094/PDIS-06-25-1164-SR

Rudra B, Gupta RS. 2024. Phylogenomics studies and molecular markers reliably demarcate genus Pseudomonas sensu stricto and twelve other Pseudomonadaceae species clades representing novel and emended genera. Front Microbiol. 14. https://doi.org/10.3389/fmicb.2023.1273665

Mielnichuk N, Bianco MI, Yaryura PM, Bertani RP, Toum L, Daglio Y, Colonnella MA, Lizarraga L, Castagnaro AP, Vojnov AA. 2021. Virulence factors analysis of native isolates of *Xanthomonas albilineans* and *Xanthomonas sacchari* from Tucumán, Argentina, reveals differences in pathogenic strategies. Plant Pathology. 2021;70:1072–1084. DOI: 10.1111/ppa.13367

Girard L, Lood C, Höfte M, Vandamme P, Rokni-Zadeh H, van Noort V, Lavigne R, De Mot R. The Ever-Expanding *Pseudomonas* Genus: Description of 43 New Species and Partition of the *Pseudomonas*

putida Group. Microorganisms. 2021 Aug 18;9(8):1766. doi: 10.3390/microorganisms9081766. PMID: 34442845; PMCID: PMC8401041.

Pagès H, Aboyoun P, Gentleman R, DebRoy S (2024). Biostrings: Efficient manipulation of biological strings. doi:10.18129/B9.bioc.Biostrings <https://doi.org/10.18129/B9.bioc.Biostrings>, R package version 2.74.1, <https://bioconductor.org/packages/Biostrings>.

Wright ES (2016). Using DECIPHER v2.0 to Analyze Big Biological Sequence Data in R. The R Journal, 8(1), 352-359

Charif D, Lobry JR. 2007. SeqinR 1.0-2: a contributed package to the R project for statistical computing devoted to biological sequences retrieval and analysis. In: Bastolla U, Porto M, Roman HE, Vendruscolo M, editors. Structural approaches to sequence evolution: molecules, networks, populations. Biological and Medical Physics, Biomedical Engineering. New York (NY): Springer-Verlag. p. 207–232.

Schliep K.P. 2011. phangorn: phylogenetic analysis in R. Bioinformatics, 27(4) 592-593

Guangchuang Yu, David Smith, Huachen Zhu, Yi Guan, Tommy Tsan-Yuk Lam. ggtree: an R package for visualization and annotation of phylogenetic trees with their covariates and other associated data. Methods in Ecology and Evolution 2017, 8(1):28-36. doi:10.1111/2041-210X.12628

Table 1. Leaf samples with Bacterial Leaf Spot (BLS)-like symptoms submitted to the Sugar Beet Plant Pathology Lab in 2024.

Sample #	Date Sampled	State	County	Township
24_23	7/28/2024	MN	Swift	Fairfield
24_24	7/28/2024	MN	Swift	Tara
24_25	7/28/2024	MN	Stevens	Moore
24_26	7/28/2024	MN	Swift	Fairfield
24_27	7/31/2024	MN	Norman	Halstad
24_28	8/1/2024	MN	Chippewa	Rheiderland
24_35	8/5/2024	MN	Mahnomen	Popple Grove
24_43	8/6/2024	MN	Renville	Osceola
24_CR	8/19/2024	MN	Polk	Lowell
24_45	8/22/2024	MN	NA[z]	NA[z]
24_46	8/22/2024	MN	Pope	Glenwood
24_47	8/22/2024	MN	NA[z]	NA[z]
24_48	8/22/2024	MN	Pope	Bangor
24_49	8/22/2024	MN	Pope	Bangor

[z] NA: not applicable as information was not provided on the field sample sheet.

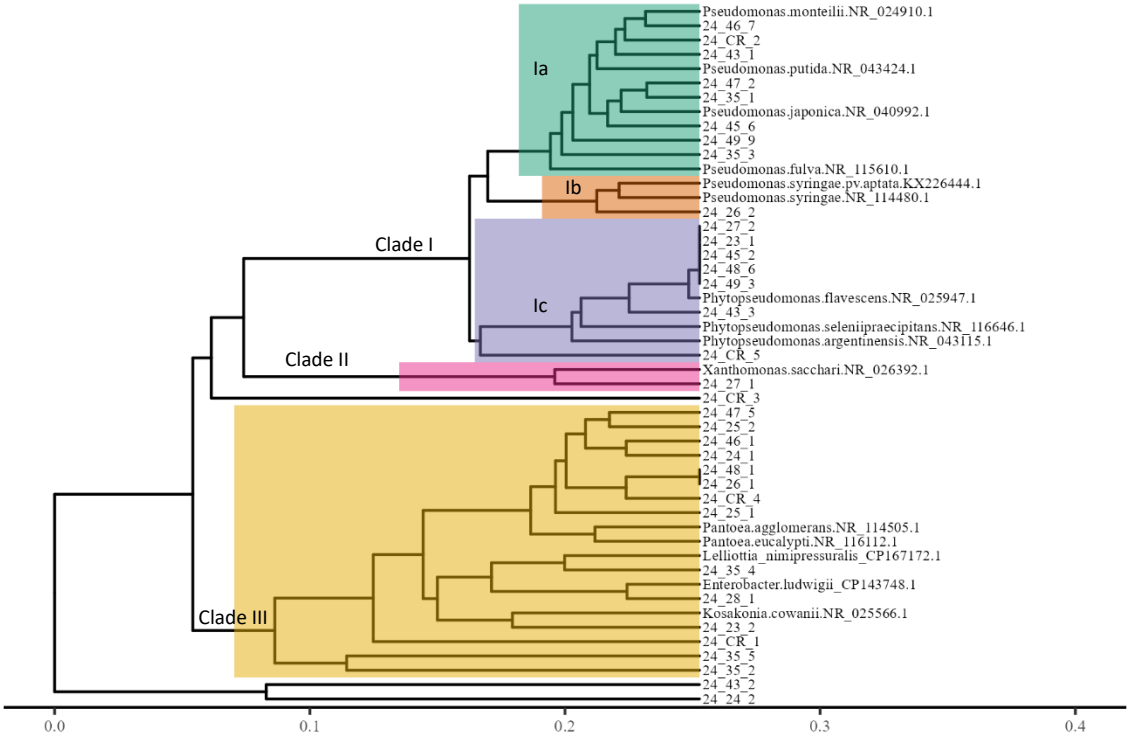

Fig 1. Preliminary phylogenetic analysis based on the *16S-23S* ribosomal RNA intergenic region.

Fig 1. Bacterial Leaf Spot (BLS)-like symptoms of field samples received in 2024 (A) and infiltration technique conducted for growth chamber pathogenicity assays (B).

Table 2. Severity and incidence of Bacterial Leaf Spot (BLS)-like symptoms on three sugar beet cultivars across 20 bacterial isolates collected from leaf samples in 2024.

Treatment	No. of infiltrations [v]	7 days after infiltration		14 days after infiltration	
		Disease severity index (0-100) [w,x]	Incidence (%) [x,y]	Disease severity index (0-100) [w,x]	Incidence (%) [x,y]
Sugar beet cultivar (main plot)					
Betaseed 8018	1641	20.1	50	29.7	68
Crystal 260	1776	18.3	50	30.7	68
Crystal 912	1737	18.5	51	28.4	68
P-value	NA	0.5069	0.9223	0.5124	0.9910
Bacterial isolate [z] (sub-plot)					
24_43_2	330	33.4 [a]	66 [a-d]	44.4 [a]	85 [a-c]
24_CR_1	310	27.2 [a-d]	64 [a-d]	43.9 [a]	85 [a-c]
24_CR_3	324	27.7 [a-c]	69 [a-c]	43.8 [a]	90 [ab]
24_46_1	316	30.0 [ab]	76 [a]	43.1 [ab]	89 [ab]
24_48_6	298	21.1 [c-h]	56 [b-e]	42.7 [ab]	87 [a-c]
24_25_2	296	26.4 [a-e]	72 [ab]	41.2 [a-c]	91 [a]
24_47_2	322	25.4 [b-f]	66 [a-d]	41.0 [a-c]	89 [ab]
24_45_6	324	23.5 [b-g]	55 [c-e]	35.2 [b-d]	83 [b-d]
24_CR_5	312	22.8 [b-h]	62 [b-d]	34.4 [cd]	85 [a-c]
24_43_3	327	16.2 [g-i]	46 [e-g]	32.3 [de]	76 [d-f]
24_35_3	143	23.2 [b-h]	60 [b-e]	30.4 [d-f]	73 [e-g]
24_24_1	141	21.6 [b-h]	58 [b-e]	30.2 [d-f]	78 [c-f]
24_35_1	160	25.0 [b-g]	74 [ab]	29.2 [d-g]	79 [c-f]
24_43_1	144	16.9 [f-i]	50 [d-f]	28.9 [d-g]	81 [b-e]
24_49_1	176	17.6 [e-i]	52 [d-f]	28.0 [d-h]	64 [g]
24_35_4	140	18.3 [d-i]	65 [a-d]	26.0 [d-h]	71 [e-g]
24_28_2	152	18.4 [c-i]	54 [c-e]	24.6 [e-h]	71 [e-g]
24_23_2	138	12.5 [h-i]	45 [e-g]	21.9 [f-h]	69 [fg]
24_35_2	129	8.4 [ij]	34 [fg]	18.3 [gh]	63 [g]
24_35_5	148	8.3 [ij]	30 [g]	16.9 [h]	49 [h]
Mock Control	524	1.7 [j]	6 [h]	3.5 [i]	14 [i]
Nontreated Control	NA	0.0 [j]	0 [h]	0.0 [i]	0 [j]
P- value	NA	**< 0.0001**	**< 0.0001**	**< 0.0001**	**< 0.0001**
Cultivar x Isolate Interactions					
P- value	NA	0.5229	0.3053	0.4345	0.2507

[v] The total number of infiltrations across one or two assays; the 10 most virulent isolates were re-evaluated.

[w] Disease severity index (DSI) was calculated by multiplying the number of infiltration sites in each severity category (0–4) by the category value, summing these products, dividing by the maximum possible score, and multiplying by 100 to standardize values from 0 to 100.

[x] Means within a column followed by a common letter are not significantly different according to the Least Significant Difference test at the 0.05 significance level.

[y] Incidence represents the percentage of infiltration sites exhibiting visible symptoms.

[z] The three-part isolate identifier corresponds to sampling year (24 = 2024), field sample number, and isolate number recovered from that sample.